Front. Earth Sci. 2018, 12(1): 86–94
https://doi.org/10.1007/s11707-017-0619-2

RESEARCH ARTICLE

The effects of sorting by aeolian processes on the geochemical characteristics of surface materials: a wind tunnel experiment

Xunming WANG (✉)[1,2], Lili LANG[1], Ting HUA[2], Caixia ZHANG[2], Hui LI[2]

1 Key Laboratory of Water Cycle & Related Land Surface Processes, Institute of Geographic Sciences and Natural Resources Research, Chinese Academy of Sciences, Beijing 100101, China
2 Key Laboratory of Desert and Desertification, Cold & Arid Regions Environmental & Engineering Research Institute, Chinese Academy of Sciences, Lanzhou 730000, China

Abstract The geochemical characteristics of aeolian and surface materials in potential source areas of dust are frequently employed in environmental reconstructions as proxies of past climate and as source tracers of aeolian sediments deposited in downwind areas. However, variations in the geochemical characteristics of these aeolian deposits that result from near-surface winds are currently poorly understood. In this study, we collected surface samples from the Ala Shan Plateau (a major potential dust source area in Central Asia) to determine the influence of aeolian processes on the geochemical characteristics of aeolian transported materials. Correlation analyses show that compared with surface materials, the elements in transported materials (e.g., Cu, As, Pb, Mn, Zn, Al, Ca, Fe, Ga, K, Mg, P, Rb, Co, Cr, Na, Nb, Si, and Zr) were subjected to significant sorting by aeolian processes, and the sorting also varied among different particle size fractions and elements. Variations in wind velocity were significantly correlated with the contents of Cr, Ga, Sr, Ca, Y, Nd, Zr, Nb, Ba, and Al, and with the Zr/Al, Zr/Rb, K/Ca, Sr/Ca, Rb/Sr, and Ca/Al ratios. Given the great variation in the geochemical characteristics of materials transported under different aeolian processes relative to those of the source materials, these results indicate that considerable uncertainty may be introduced to analyses by using surface materials to trace the potential source areas of aeolian deposits that accumulate in downwind areas.

Keywords aeolian process, transported material, geochemistry

Received August 4, 2016; accepted September 17, 2016

E-mail: xunming@igsnrr.ac.cn

1 Introduction

The transport routes taken by aeolian deposits from their potential mineral dust source areas have been documented previously, and pedogenesis effects, post-depositional weathering, and variations in their geochemical characteristics from source to deposition have been used to indicate regional environmental change (Harrison et al., 2001; Larrasoaña et al., 2003). At present, dust emissions from Central Asia (e.g., Stevens et al., 2010; Pullen et al., 2011) are considered the source of loess (e.g., Liu, 1985) and particles in ice cores (e.g., Bory et al., 2003), and yield evidence on atmospheric circulation and past climate change (Hao and Guo, 2005; Sun et al., 2010).

After being subjected to post-depositional weathering that may have influenced their particle size and geochemistry, aeolian deposits have been employed as proxies of variations in the intensity of Asian monsoons (Chen et al., 2007), and of precipitation, wind regimes, and chemical weathering (Maher and Thompson, 1991; Yancheva et al., 2007; Jeong et al., 2011). For instance, by examining fluctuations in the concentrations of elements in snowpit samples, Huang et al. (2013) suggested that Cu, Zn, Cd, Hg, and Pb originated from remote regions. By analyzing surface soil samples, Hao et al. (2010) showed that the TiO_2/Al_2O_3 ratio is a useful indicator of the sources of loess deposits in southern China. Furthermore, Chen et al. (2006) proposed that the Zr/Rb ratios of sequences are sensitive to loess–paleosol alternations, while Sun and Zhu (2010) suggested that the observed decrease in concentrations of Cr, Cu, Co, Zn, and Ni in samples reflected variations in the detrital source. Rodrigo-Gámiz et al. (2011) reported that increases in aeolian proxies, such as the Zr/Al, Si/Al, and Ti/Al ratios, indicate dryer conditions,

while Weiss et al. (2002) found that the concentration profiles of Mn, Sr, and Ca reflected the influence of chemical diagenesis on underlying sediments. Ferrat et al. (2012) showed that the vertical distributions of Al, Ti, Sr, and Ca could be employed to indicate the degree of influence of groundwater on element concentrations, and that rare earth element and trace element ratios are useful indicators of changing dust sources. In addition, Taylor and McLennan (1985) and Lawrence and Neff (2009) suggested that, with the exception of Na and sometimes Ca, the geochemical composition of dust resembled the composition of the upper continental crust for most major elements, while Lawrence et al. (2013) reported that the concentrations of elements such as Cd, Zn, Pb, and Cu indicate that the accumulation of some elements in soil is beyond what can be explained by local rock weathering. Although these aeolian deposits have been widely used as proxies in paleoclimate reconstructions, aeolian activity has fluctuated considerably in the potential source areas throughout the Quaternary (e.g., Sun et al., 2010), which may have caused variations in both the contents and compositions of aeolian materials, with consequent effects on the resolution and precision of paleoclimate reconstructions in downwind areas.

In addition, by comparing the geochemical characteristics of surface materials sampled in the potential dust source areas with those of aeolian deposits in downwind areas, researchers have identified the potential source areas of the deposits (e.g., Li et al., 2007; Rao et al., 2008; Yang et al., 2009; Chen and Li, 2011). However, a recent study has attributed considerable variations in the composition of Aeolian-transported materials to variations in the strength of aeolian processes in the potential source areas of dust (Wang et al., 2015). There is little information about the nature of variations in the characteristics of aeolian deposits attributable to variable near-surface wind strengths. It is therefore important to gain an improved understanding of the geochemical characteristics of aeolian-transported materials, so as to identify the sources of materials that form aeolian deposits. In this study, therefore, we simulated the effects of aeolian processes on typical surface source samples collected from potential dust source areas in a series of wind-tunnel experiments to determine the geochemical characteristics of transported materials, to examine the influence of aeolian processes on the geochemical characteristics of aeolian-transported materials, and to verify the degree of uncertainty associated with using surface materials to trace potential dust sources areas of aeolian deposits.

2 Sampling sites, wind tunnel experiments, and analytical methods

The sampling sites were located on the Ala Shan Plateau, an extremely arid area of the Inner Mongolian Plateau, Central Asia (Fig. 1). A more detailed description of the study environment has been provided by Wang et al. (2012a). This region is a potential source of highly concentrated dust emissions (e.g., Wang et al., 2008) that have been detected as loess and as aeolian material in ice cores and lakes (e.g., Maher, 2011). We collected 15 bulk surface samples from areas with no vegetation cover, no biological or physical soil crusts, no human disturbance, and with similar gravel coverage in each case. We conducted wind-tunnel experiments at the Key Laboratory of Desert and Desertification of the Cold and Arid Regions Environmental and Engineering Research Institute at the

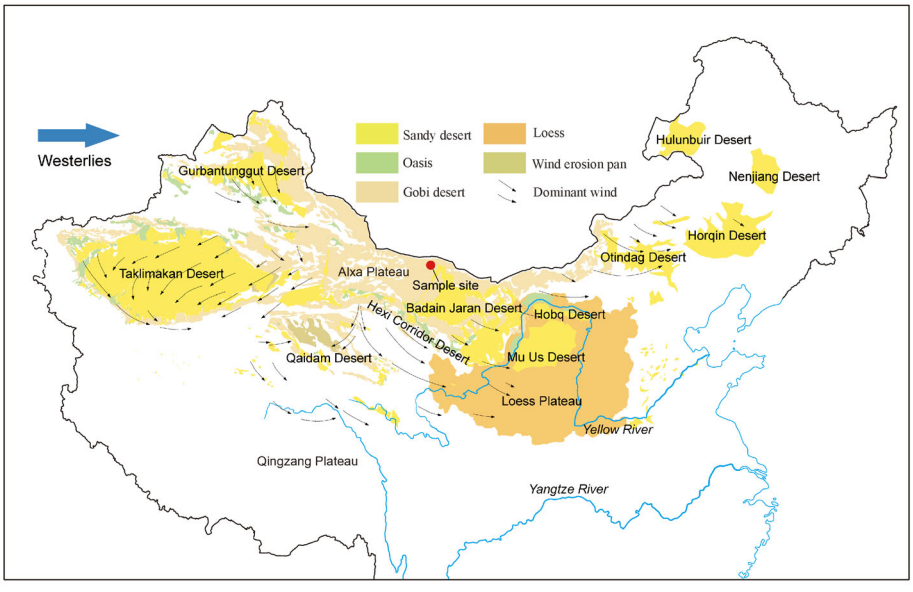

Fig. 1 Aeolian geomorphology of Central Asia and sampling sites. Data are from the Environmental and Ecological Science Data Center for West China, National Natural Science Foundation of China (http://westdc.westgis.ac.cn).

Chinese Academy of Sciences, Lanzhou, Gansu Province, China. Further details of the wind tunnel have been provided in previous papers (e.g., Dong et al., 2004, 2007). The experimental equipment is illustrated in Fig. 2, and details of the methods are provided by Wang et al. (2012b). In brief, a layer of each sample, about 2 cm thick, was spread out in the working section of the wind tunnel. At a distance of 30 cm downwind from the sample, a dust collector, 30 cm high and the same width as the surface samples, was installed downwind to collect transported materials. Earlier test results indicated that the sampler collects more than 95% of the transported materials. To simulate the variations in near-surface wind velocity, the experiments were conducted with an initial free-stream wind velocity of 8 m/s; the velocity was then progressively increased to 22 m/s in 2 m/s increments. For each run, we stopped the sampling and collected materials in the sampler until the surface particles were no longer moving. In the experiments, sediment transport ceased within 360 and 60 s at wind velocities of 8 m/s and 22 m/s, respectively.

The transported materials were collected from the dust collector once the experiment had ended. The particle size distribution of the transported material was determined with a laser particle size analyzer (Mastersizer 2000, Malvern Instruments, Malvern, UK). Concentrations of 26 elements and oxides (SiO_2, Al_2O_3, Fe_2O_3, MgO, CaO, Na_2O, K_2O, P, Ti, V, Cr, Mn, Co, Ni, Cu, Zn, Ga, As, Rb, Sr, Y, Zr, Nb, Ba, Ce, and Pb) were determined by a fully automated sequential wavelength-dispersive X-ray fluorescence (XRF) spectrometer (AXIOS, PANalytical) equipped with a Super Sharp Tube for the Rh-anode, with settings of 4.0 kW, 60 kV, 160 mA, and a 75 μ UHT Be end-window. Details of the sample preparation, calibration of element concentrations, and analytical uncertainties have been described by Wang et al. (2012c, 2015). In addition, because a stronger wind will transport not only the material that can actually be transported at that wind velocity but also all the other material that can be transported at lower wind velocities, we express all the particle size fractions and elemental concentrations at a given wind velocity as the weighted average values for the materials collected at that wind velocity and all lower velocities (Wang et al., 2012b). Therefore, the values presented are the virtual values at each given wind velocity.

3 Results and discussion

Particle size distributions of the surface and transported materials under different wind velocities are shown in Fig. 3. There were some differences among the particle size distributions of the surface and transported materials, which indicate that aeolian processes can result in considerable sorting of the surface materials. In addition, the results of correlation analysis between the particle size fractions and the element concentrations of the source surface material and transported materials are presented in Table 1. There were no significant correlations between the particle size fractions and the elemental concentrations of the surface materials, except for As, Cu, Mn, Pb, and Zn, which indicates that most elements were poorly sorted in the surface samples. The differences in sorting may reflect variations in the parent materials of these elements (e.g., Kasper-Zubillaga et al., 2007). However, compared with the surface materials, the transported materials were strongly sorted by aeolian processes (e.g., Livingstone et al., 1999; Kasper-Zubillaga et al., 2013) and there were variations in the degree of sorting of different particle size

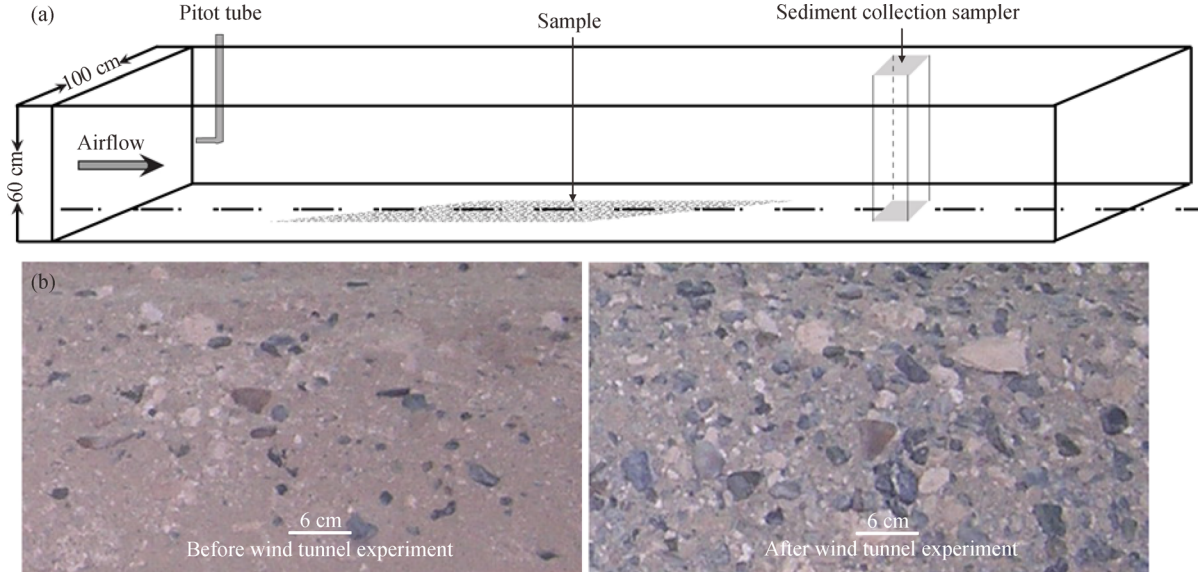

Fig. 2 Schematic diagram of (a) surface samples, and (b) the wind-tunnel and sampling setup during the wind-tunnel experiments.

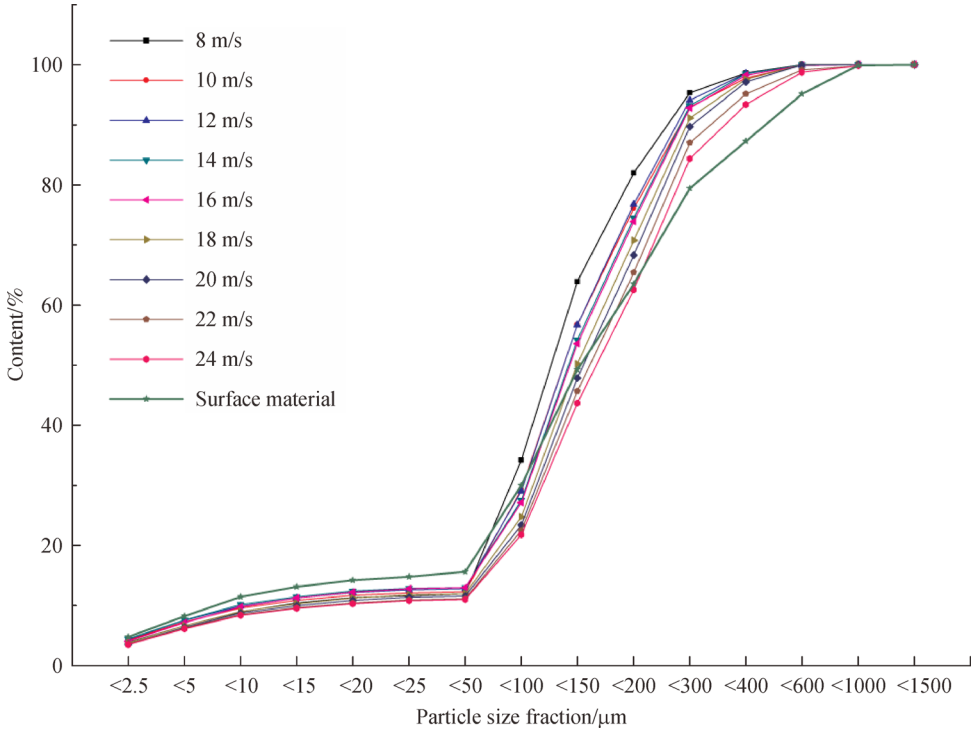

Fig. 3 Cumulative contents (%) of the different particle-size fractions of the surface and transported materials under different wind velocities.

Table 1 Comparisons of correlation coefficient between elemental concentrations and the different particle-size fractions of the transported and surface materials. Significant correlations are marked in bold

Elemental concentrations		< 2.5 μm	< 10 μm	< 20 μm	< 50 μm	< 200 μm	> 200 μm
Al_2O_3	Surface material	.502	.502	.479	.393	−.082	.082
	Transported material	**.664****	**.640****	**.616****	**.593****	−.027	.027
As	Surface material	**.662***	**.682***	**.672***	**.608***	193	−.193
	Transported material	**.759****	**.771****	**.771****	**.765****	**.368****	**−.368****
Ba	Surface material	.154	.148	.137	.092	−.399	.399
	Transported material	**.307****	**.280****	**.255***	.214	**−.245***	**.245***
CaO	Surface material	.405	.452	.473	.474	.538	−.538
	Transported material	**.256***	**.276***	**.295****	**.277***	**.407****	**−.407****
Ce	Surface material	−.015	−.051	−.058	−.064	.355	−.355
	Transported material	−.162	−.155	−.141	−.087	**.330****	**−.330****
Co	Surface material	−.264	−.311	−.324	−.328	−.039	.039
	Transported material	**−.353****	**−.360****	**−.358****	**−.336****	−.058	.058
Cr	Surface material	−.123	−.117	−.110	−.100	.475	−.475
	Transported material	**−.270***	**−.267***	**−.262***	−.209	**.366****	**−.366****
Cu	Surface material	**.767****	**.780****	**.767****	**.724***	.318	−.318
	Transported material	**.807****	**.794****	**.786****	**.818****	**.257***	**−.257***
Fe_2O_3	Surface material	.410	.420	.415	.387	.506	−.506
	Transported material	**.265***	**.260***	**.258***	**.310****	**.456****	**−.456****
Ga	Surface material	.223	.242	.227	.139	−.014	.014
	Transported material	**.626****	**.599****	**.574****	**.563****	−.057	.057

(*Continued*)

Elemental concentrations		< 2.5 μm	< 10 μm	< 20 μm	< 50 μm	< 200 μm	> 200 μm
K_2O	Surface material	.177	.166	.142	.063	−.306	.306
	Transported material	**.481****	**.448****	**.422****	**.402****	−.142	.142
MgO	Surface material	.475	.487	.487	.505	.409	−.409
	Transported material	**.465****	**.506****	**.534****	**.556****	**.512****	**−.512****
Mn	Surface material	**.684***	**.685***	**.672***	**.618***	.284	−.284
	Transported material	**.661****	**.660****	**.653****	**.672****	**.351****	**−.351****
Na_2O	Surface material	−.352	−.346	−.336	−.313	−.266	.266
	Transported material	**−.240***	−.213	−.202	**−.240***	**−.242***	**.242***
Nb	Surface material	−.018	−.011	−.005	−.014	.544	−.544
	Transported material	**−.232***	**−.221***	−.214	−.164	**.444****	**−.444****
Nd	Surface material	.155	.168	.170	.153	.534	−.534
	Transported material	−.203	−.181	−.169	−.125	**.464****	**−.464****
Ni	Surface material	.349	.356	.362	.383	.537	−.537
	Transported material	.007	.022	.037	.102	**.434****	**−.434****
Pb	Surface material	**.846****	**.866****	**.857****	**.821****	.100	−.100
	Transported material	**.720****	**.718****	**.709****	**.698****	.051	−.051
P	Surface material	.442	.452	.457	.460	.600	−.600
	Transported material	**.415****	**.434****	**.442****	**.506****	**.476****	**−.476****
Rb	Surface material	.535	.550	.542	.507	.350	−.350
	Transported material	**.604****	**.599****	**.593****	**.636****	**.288****	**−.288****
SiO_2	Surface material	−.439	−.488	−.505	−.508	−.379	.379
	Transported material	**−.340****	**−.369****	**−.390****	**−.353****	**−.273***	**.273***
Sr	Surface material	−.149	−.125	−.120	−.154	−.228	.228
	Transported material	.004	−.009	−.013	−.082	−.207	.207
Ti	Surface material	.018	.022	.023	−.012	.568	−.568
	Transported material	−.120	−.118	−.120	−.084	**.456****	**−.456****
V	Surface material	.180	.186	.182	.149	.486	−.486
	Transported material	.063	.053	.048	.093	**.426****	**−.426****
Y	Surface material	−.050	−.044	−.043	−.079	.519	−.519
	Transported material	−.151	−.141	−.136	−.089	**.452****	**−.452****
Zn	Surface material	**.851****	**.885****	**.880****	**.835****	.390	−.390
	Transported material	**.576****	**.582****	**.580****	**.576****	**.263***	**−.263***
Zr	Surface material	−.367	−.353	−.346	−.365	.419	−.419
	Transported material	**−.394****	**−.390****	**−.387****	**−.358****	**.367****	**−.367****

*Correlation is significant at the 0.05 level (2-tailed).
**Correlation is significant at the 0.01 level (2-tailed).

fractions and elements, which suggests that caution must be exercised when surface materials are used to trace the potential source areas of aeolian deposits. For example, in addition to the elements mentioned above, the concentrations of Fe, Ga, K, Mg, Al, Ba, Ca, P, and Rb were significantly and positively correlated, and concentrations of Co, Cr, Na, Nb, Si, and Zr were significantly and negatively correlated, with the fine fractions of the aeolian-transported materials. These results show that thorough sorting of grains during aeolian processes results in considerable differences in the composition of both the surface and transported materials. This result reinforces the need to carefully consider each particular situation before using the element compositions of surface materials collected in potential dust source areas to trace the source of aeolian sediments of downwind areas.

Variations in wind velocities also resulted in large differences in the contents or ratios of some elements in the aeolian-transported materials (Table 2). For instance, there were significant positive correlations between wind velocity and the Cr, Ga, Sr, Y, Zr, Nb, Ba, Nd, and Al contents, and the Zr/Al, Zr/Rb, K/Ca, and Sr/Ca ratios, and significant negative correlations between wind velocity and Ca contents, and the Rb/Sr and Ca/Al ratios (Fig. 4 and Table 2). Variations in near-surface winds that occurred in different periods in the potential dust source areas may therefore have changed the composition of transported materials, thereby resulting in variations in the element ratios of aeolian sediments, with possible consequences for the resolution and precision of paleoclimate reconstructions in downwind areas.

Furthermore, as the intensities of the aeolian processes varied, the particle size class composition of the transported materials also varied. For instance, as the wind velocity increased, the total contents of the fine fractions with a diameter of < 50 μm decreased, and the coarse fractions with a diameter of > 200 μm increased (Fig. 5). Because the stratigraphic sequences in downwind areas consist mainly of the fine fractions of the transported materials, variations in the contents of the fine fractions suggest that the resolution and precision of proxies of past climate reconstructions based on these materials may also be greatly influenced by variations in aeolian processes in potential source areas of dust.

4 Conclusions

Variations in aeolian processes result in significant differences between the contents of the fine fractions and the geochemical characteristics of aeolian-transported materials. Correlation analyses revealed that aeolian processes had a significant influence on sorting of the elements associated with the fine fractions of transported materials, such as As, Cu, Mn, Pb, Zn, Al, Ca, Fe, Ga, K, Mg, P, Rb, Co, Cr, Na, Nb, Si, and Zr. Wind velocity was significantly correlated with the contents of Cr, Ga, Sr, Y, Zr, Nb, Ba, Nd, and Al, and the ratios of Zr/Al, Zr/Rb, K/Ca, Sr/Ca, Ca, Rb/Sr, and Ca/Al. These results show that variations in aeolian processes in potential source areas of dust may influence the composition of transported materials; consequently, the application of surface

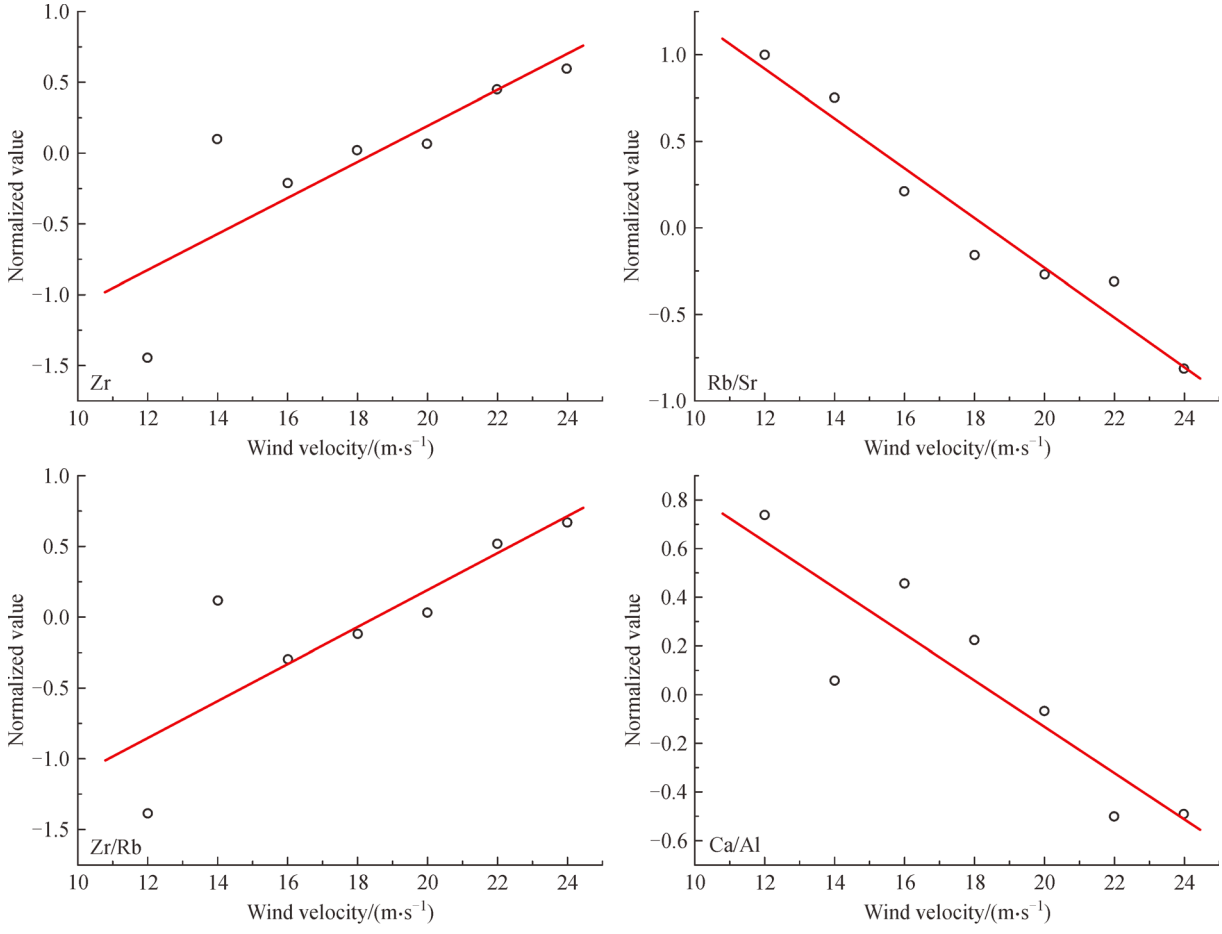

Fig. 4 Concentrations of selected elements and ratios in transported materials (average values of the 15 surface samples) at different wind velocities.

Table 2 Pearson correlations between wind velocity and elemental concentrations of the transported materials. Significant correlations are marked in bold

Element (Ratio)	P	Ti	V	Cr	Mn	Co	Ni	Cu
Correlation	.114	.124	−.034	**.244***	.059	−.042	.022	.111
Element (Ratio)	Zn	Ga	As	Rb	Sr	Y	Zr	Nb
Correlation	−.011	**.386****	−.019	.108	**.365****	**.451****	**.485****	**.500****
Element (Ratio)	Ba	Ce	Nd	Pb	SiO_2	Al_2O_3	Fe_2O_3	MgO
Correlation	**.226***	−.113	**.237***	.116	.056	**.353****	−.190	−.124
Element (Ratio)	CaO	Na_2O	K_2O	Na_2O/CaO	Si/Al	Zr/Al	Rb/Sr	Sr/Ba
Correlation	**–.272***	−.139	.153	.163	.004	**.463****	**–.547****	.005
Element (Ratio)	Zr/Rb	Mg/Al	Ca/Al	K/Ca	Sr/Ca			
Correlation	**.478****	−.158	**–.323****	**.272***	**.522****			

*Correlation is significant at the 0.05 level (2-tailed).

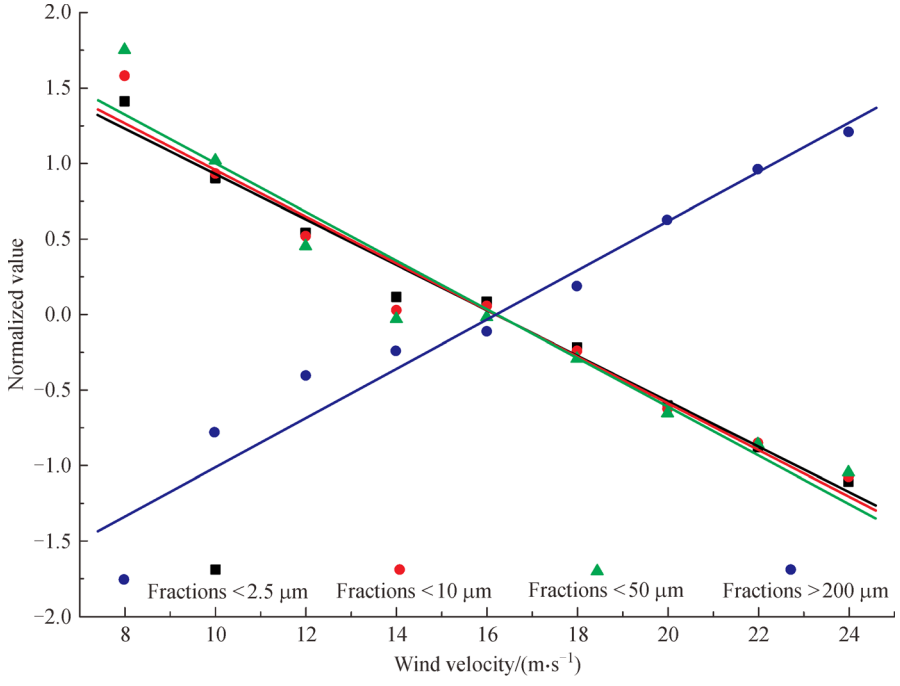

Fig. 5 Contents of different particle classes of transported materials (average values of the 15 surface samples) at different wind velocities.

materials to trace the potential source areas of aeolian deposits must be treated with caution. Variations in the geochemical characteristics of transported materials may affect the resolution and precision of paleoclimate reconstructions in downwind areas if the sorting effects of near-surface winds are not carefully appraised.

Acknowledgements This work was supported by the National Key Research and Development Program of China (No. 2016YFA0601900), grants from the National Natural Science Foundation of China (Grant Nos. 41225001 and 41401005), and the Foundation of the Director of the Institute of Geographic Sciences and Natural Resources Research, Chinese Academy of Sciences. Special thanks are given to anonymous referees and the journal editor for constructive criticism of an earlier version of this manuscript.

References

Bory A J M, Biscaye P E, Grousset F E (2003). Two distinct seasonal Asian source regions for mineral dust deposited in Greenland (NorthGRIP). Geophys Res Lett, 30(4): 1167

Chen J, Chen Y, Liu L, Ji J, Balsam W, Sun Y, Lu H (2006). Zr/Rb ratio in the Chinese loess sequences and its implication for changes in the East Asian winter monsoon strength. Geochim Cosmochim Acta, 70

(6): 1471–1482

Chen J, Li G, Yang J, Rao W, Lu H, Balsam W, Sun Y, Ji J (2007). Nd and Sr isotopic characteristics of Chinese deserts: implications for the provenances of Asian dust. Geochim Cosmochim Acta, 71(15): 3904–3914

Chen J, Li G J (2011). Geochemical studies on the source region of Asian dust. Sci China Earth Sci, 54(9): 1279–1301

Dong Z, Qian G, Luo W, Wang H (2007). A wind tunnel simulation of the effects of stoss slope on the lee airflow pattern over a two-dimensional transverse dune. J Geophys Res, 112(F3): F03019

Dong Z, Wang H, Liu X, Wang X (2004). The blown sand flux over a sandy surface: a wind tunnel investigation on the fetch effect. Geomorphology, 57(1−2): 117–127

Ferrat M, Weiss D J, Spiro B, Large D (2012). The inorganic geochemistry of a peat deposit on the eastern Qinghai-Tibetan Plateau and insights into changing atmospheric circulation in central Asia during the Holocene. Geochim Cosmochim Acta, 91: 7–31

Hao Q, Guo Z, Qiao Y, Xu B, Oldfield F (2010). Geochemical evidence for the provenance of middle Pleistocene loess deposits in southern China. Quat Sci Rev, 29(23−24): 3317–3326

Hao Q Z, Guo Z T (2005). Spatial variations of magnetic susceptibility of Chinese loess for the last 600 kyr: implications for monsoon evolution. J Geophys Res, 110(B12): B12101

Harrison S P, Kohfeld K E, Roelandt C, Claquin T (2001). The role of dust in climate changes today, at the last glacial maximum and in the future. Earth Sci Rev, 54(1−3): 43–80

Huang J, Kang S, Zhang Q, Guo J, Chen P, Zhang G, Tripathee L (2013). Atmospheric deposition of trace elements recorded in snow from the Mt. Nyainqêntanglha region, southern Tibetan Plateau. Chemosphere, 92(8): 871–881

Jeong G Y, Hillier S, Kemp R A (2011). Changes in mineralogy of loess–paleosol sections across the Chinese Loess Plateau. Quat Res, 75(1): 245–255

Kasper-Zubillaga J J, Armstrong-Altrin J S, Carranza-Edwards A, Morton-Bermea O, Lozano Santa Cruz R (2013). Control in beach and dune sands of the Gulf of Mexico and the role of nearby rivers. International Journal of Geosciences, 4(08): 1157–1174

Kasper-Zubillaga J J, Zolezzi-Ruiz H, Carranza-Edwards A, Girón-García P, Ortiz-Zamora G, Palma M (2007). Sedimentological, modal analysis and geochemical studies of desert and coastal dunes, Altar Desert, NW México. Earth Surf Process Landf, 32(4): 489–508

Larrasoaña J C, Roberts A P, Rohling E J, Winklhofer M, Wehausen R (2003). Three million years of monsoon variability over the northern Sahara. Clim Dyn, 21: 689–698

Lawrence C R, Neff J C (2009). The contemporary physical and chemical flux of aeolian dust: a synthesis of direct measurements of dust deposition. Chem Geol, 267(1−2): 46–63

Lawrence C R, Reynolds R L, Ketterer M E, Neff J C (2013). Aeolian controls of soil geochemistry and weathering fluxes in high-elevation ecosystems of the Rocky Mountains, Colorado. Geochim Cosmochim Acta, 107: 27–46

Li G, Chen J, Chen Y, Yang J, Ji J, Liu L (2007). Dolomite as a tracer for the source regions of Asian dust. J Geophys Res, D, Atmospheres, 112(D17): D17201

Liu T (1985). Loess and Environments. Beijing: China Ocean Press, 251

Livingstone I, Bullard J E, Wiggs G F S, Thomas D S G (1999). Grain-size variation on dunes in the southwest Kalahari, Southern Africa. J Sediment Res, 69(3): 546–552

Maher B A (2011). The magnetic properties of Quaternary aeolian dusts and sediments, and their palaeoclimatic significance. Aeolian Res, 3 (2): 87–144

Maher B A, Thompson R (1991). Mineral magnetic record of the Chinese loess and paleosols. Geology, 19(1): 3–6

Pullen A, Kapp P, McCallister A T, Chang H, Gehrels G E, Garzione C N, Heermance R V, Ding L (2011). Qaidam Basin and northern Tibetan Plateau as dust sources for the Chinese Loess Plateau and paleoclimatic implications. Geology, 39(11): 1031–1034

Rao W B, Chen J, Yang J D, Ji J F, Li G J, Tan H B (2008). Sr-Nd isotopic characteristics of eolian deposits in the Erdos Desert and Chinese Loess Plateau: implications for their provenances. Geochem J, 42(3): 273–282

Rodrigo-Gámiz M, Martínez-Ruiz F, Jiménez-Espejo F J, Gallego-Torres D, Nieto-Moreno V, Romero O, Ariztegui D (2011). Impact of climate variability in the western Mediterranean during the last 20,000 years: oceanic and atmospheric responses. Quat Sci Rev, 30 (15−16): 2018–2034

Stevens T, Palk C, Carter A, Lu H, Clift P D (2010). Assessing the provenance of loess and desert sediments in northern China using U-Pb dating and morphology of detrital zircons. Geol Soc Am Bull, 122 (7−8): 1331–1344

Sun J, Zhu X (2010). Temporal variations in Pb isotopes and trace element concentrations within Chinese eolian deposits during the past 8 Ma: implications for provenance change. Earth Planet Sci Lett, 290(3−4): 438–447

Sun Y B, Wang X, Liu Q, Clemens S (2010). Impacts of post-depositional processes on rapid monsoon signals recorded by the last glacial loess deposits of northern China. Earth Planet Sci Lett, 289(1−2): 171–179

Taylor S R, McLennan S M (1985). The Continental Crust: Its Composition and Evolution. Oxford: Blackwell Scientific Publication, 312

Wang X, Lang L, Hua T, Wang H, Zhang C, Wang Z (2012a). Characteristics of the Gobi desert and their significance for dust emissions in the Ala Shan Plateau (Central Asia): an experimental study. J Arid Environ, 81: 35–46

Wang X, Lang L, Hua T, Zhang C, Xia D (2015). Geochemical and magnetic characteristics of aeolian transported materials under different near-surface wind fields: an experimental study. Geomorphology, 239: 106–113

Wang X, Lang L, Zhang C, Hua T, Wang H (2012b). The influence of near-surface winds on Sr isotope composition of aeolian sediments: a wind tunnel experiment. Chem Geol, 308–309: 10–17

Wang X, Xia D, Wang T, Xue X, Li J (2008). Dust sources in arid and semiarid China and southern Mongolia: impacts of geomorphological setting and surface materials. Geomorphology, 97(3−4): 583–600

Wang X, Xia X, Zhang C, Lang L, Hua T, Zhao S (2012c). Geochemical and magnetic characteristics of fine-grained surface sediments in potential dust source areas: implications for tracing the provenance of aeolian deposits and associated palaeoclimatic change in East Asia.

Palaeogeogr Palaeoclimatol Palaeoecol, 323–325: 123–132

Weiss D, Shotyk W, Rieley J, Page S, Gloor M, Reese S, Martinez-Cortizas A (2002). The geochemistry of major and selected trace elements in a forested peat bog, Kalimantan, SE Asia, and its implications for past atmospheric dust deposition. Geochim Cosmochim Acta, 66(13): 2307–2323

Yancheva G, Nowaczyk N R, Mingram J, Dulski P, Schettler G, Negendank J F W, Liu J, Sigman D M, Peterson L C, Haug G H (2007). Influence of the intertropical convergence zone on the East Asian monsoon. Nature, 445(7123): 74–77

Yang J, Li G, Rao W, Ji J (2009). Isotopic evidences for provenance of East Asian Dust. Atmos Environ, 43(29): 4481–4490